High-pressure x-ray and neutron powder diffraction study of $PbWO_4$ and $BaWO_4$ scheelites

2006 J. Phys.: Condens. Matter 18 3017

(http://iopscience.iop.org/0953-8984/18/11/008)

INSTITUTE OF PHYSICS PUBLISHING JOURNAL OF PHYSICS: CONDENSED MATTER

J. Phys.: Condens. Matter **18** (2006) 3017–3029 doi:10.1088/0953-8984/18/11/008

High-pressure x-ray and neutron powder diffraction study of $PbWO_4$ and $BaWO_4$ scheelites

Andrzej Grzechnik[1,4], **Wilson A Crichton**[2], **William G Marshall**[3] **and Karen Friese**[1]

[1] Departamento de Física de la Materia Condensada, Universidad del País Vasco, Apartado 644, Bilbao, E-48080, Spain
[2] European Synchrotron Radiation Facility, BP 220, F-38043 Grenoble cedex, France
[3] ISIS Neutron Facility, Rutherford Appleton Laboratory, Chilton, Didcot, Oxon OX11 0QX, UK

E-mail: andrzej@wm.lc.ehu.es

Received 7 November 2005
Published 27 February 2006
Online at stacks.iop.org/JPhysCM/18/3017

Abstract

The room-temperature high-pressure behaviour of $PbWO_4$ and $BaWO_4$ scheelites ($I4_1/a$, $Z = 4$) has been studied with synchrotron angle-dispersive x-ray powder diffraction in a diamond anvil cell and time-of-flight neutron powder diffraction in a large-volume Paris–Edinburgh cell. Full profile Rietveld refinements of the neutron data provide evidence for distinct compressibility mechanisms in these materials. The distortion in the anionic array from the ideal fluorite packing in $BaWO_4$ increases upon compression while it decreases in $PbWO_4$.

(Some figures in this article are in colour only in the electronic version)

1. Introduction

Lead and barium tungstates belong to the family of ABO_4 compounds (A: Ca, Sr, Ba, Pb; B: W, Mo) that are used as laser host materials and ionic conductors [1]. Among them, $PbWO_4$ is one of the most studied scintillating materials due to its applications in the detectors for high-energy physics accelerators [1]. The ABO_4 compounds could be optimized to have higher scintillation efficiency not only by multiple ion doping but also by inducing stress and/or non-stoichiometry. To understand the structural (in)stabilities and distortions in these compounds, further studies under different pressure–temperature conditions are thus warranted.

Under ambient conditions, $PbWO_4$-I stolzite and $BaWO_4$-I have the $CaWO_4$ scheelite structure ($I4_1/a$, $Z = 4$), which is a superstructure of fluorite CaF_2 ($Fm\bar{3}m$, $Z = 4$). In both materials, the Pb^{2+}/Ba^{2+} and W^{6+} cations are eightfold and fourfold coordinated by oxygens, respectively. The structure of $PbWO_4$-II raspite ($P2_1/a$, $Z = 4$) consists of chains of edge-sharing, nearly regular WO_6 octahedra which run parallel to the y axis with the divalent

[4] Author to whom any correspondence should be addressed.

Pb cations occupying the interstitial sites and being coordinated to seven oxygen anions [2]. $PbWO_4$-II irreversibly transforms to $PbWO_4$-I above 673 K at ambient pressure. The topotactic relation between the two structures is $a_{II} = -b_I + c_I$, $b_{II} = a_I$, and $c_{II} = b_I$.

Reversible first-order phase transitions in $BaWO_4$-I and $PbWO_4$-I occurring at 6.5 and 4.5 GPa, respectively, have previously been studied with Raman scattering [3, 4]. Raman bands abruptly shift to lower energies during these phase transformations without any anomalies such as those observed in $CaWO_4$ and $SrWO_4$ [5]. Jayaraman *et al* [3] have postulated that the coordination of tungstate atoms in the high-pressure polymorphs of $BaWO_4$-I becomes octahedral and the structure is of the $HgWO_4$ type ($C2/c$, $Z = 4$), consisting of zigzag chains of edge-sharing WO_6 octahedra running along the c axis and layers of very distorted corner-sharing HgO_6 octahedra in the bc plane. However, Panchal *et al* [6] have recently shown that the structure of $BaWO_4$ stable above about 7 GPa is of the fergusonite type ($I2/a$, $Z = 4$), which is a distorted variant of scheelite. The scheelite $\rightarrow$ fergusonite phase transition has also been observed in $CaWO_4$ [7] and $CaMoO_4$ [8] using synchrotron angle-dispersive x-ray powder diffraction. Above 10 GPa, $SrWO_4$ transforms to the fergusonite structure with no significant volume collapse [9]. However, the compression data including both phases of strontium tungstate cannot be fitted by a common Birch–Murnaghan equation of state. An onset of decomposition into component oxides SrO and WO_3 occurs at about 15 GPa and the pressure-induced transformations are irreversible. The results of Raman scattering measurements in related $BaMoO_4$ by Christofilos *et al* [10] indicate that the tetrahedral units MoO_4^{2-} are preserved in its high-pressure phase above about 6 GPa.

The high-pressure high-temperature forms of $BaWO_4$ [11] and $PbWO_4$ [12] are monoclinic ($BaWO_4$-II or $PbWO_4$-III, $P2_1/n$, $Z = 8$) with no resemblance to the scheelite, fergusonite, raspite, or $HgWO_4$ types. They consist of densely packed layers of WO_6 octahedra connected by edges and corners. Barium or lead atoms, respectively, located between the layers are distributed over two non-equivalent crystallographic sites with the coordination numbers of Ba being 9 and 8 [11] and the coordination numbers of both sets of Pb atoms being 8 [12]. $BaWO_4$-II [11] can be obtained at pressures of 4–5 GPa and temperatures of 873–1273 K, $P(\text{GPa}) = 1.95 + 0.00265T$ (K). $PbWO_4$-III [12] has been synthesized at 1.5–2.5 GPa and 623–923 K, $P(\text{GPa}) = -1.0 + 0.0039T$ (K). It is unclear whether $BaWO_4$-II and $PbWO_4$-III are in any way related to the phases observed *in situ* above 6.5 and 4.5 GPa, respectively [5, 6], at room temperature. Theoretical calculations by Li *et al* [13] suggest that $PbWO_4$-II raspite ($P2_1/a$, $Z = 4$) is more stable than $PbWO_4$-I stolzite ($I4_1/a$, $Z = 4$) at ambient pressure. Raspite is supposed to transform to $PbWO_4$-III ($P2_1/n$, $Z = 8$) at 1.8 GPa.

In this study, we report on high-pressure behaviours of $PbWO_4$ and $BaWO_4$ scheelites at room temperature studied with synchrotron angle-dispersive x-ray powder diffraction in a diamond anvil cell and time-of-flight neutron powder diffraction in a large-volume Paris–Edinburgh cell. The structural parameters from the Rietveld refinements of neutron data are analysed in terms of polyhedral compressibilities. The main goal of this study is to investigate structural deformations in these materials with a novel approach in high-pressure crystallography using pseudosymmetry [14, 15], applied here to measure relative distortions in the scheelite superstructure of the fluorite type. We discuss all our observations in relation to the systematics of the ABX_4-type compounds.

2. Experimental details

Finely ground samples of polycrystalline $PbWO_4$ and $BaWO_4$ scheelites (both 99.9%, Chempur Feinchemikalien und Forschungsbedarf, Karlsruhe) were used for all high-pressure experiments.

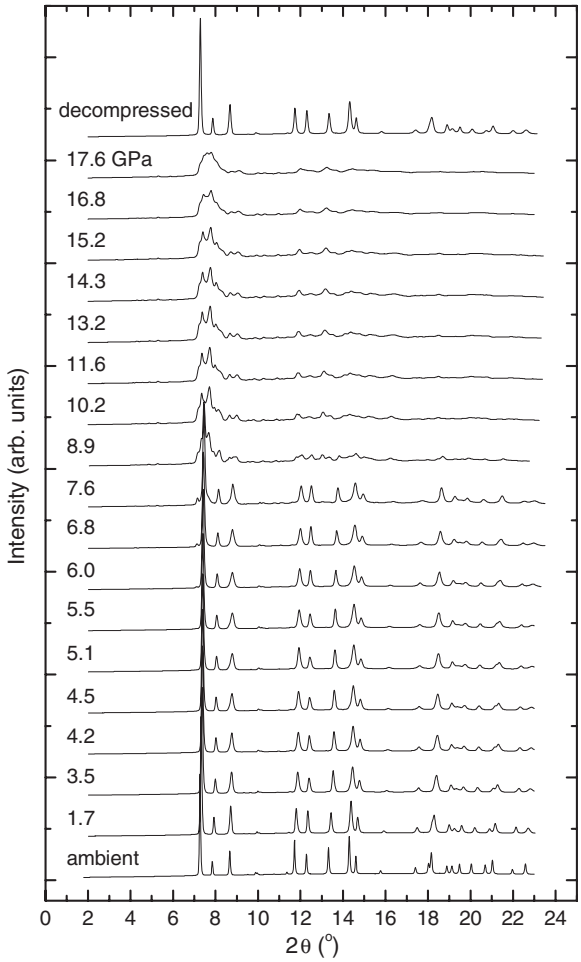

Figure 1. X-ray powder patterns of $PbWO_4$ at high pressures ($\lambda = 0.4133$ Å). The numbers stand for pressures in GPa.

Angle-dispersive x-ray powder diffraction patterns of $PbWO_4$ were measured in a diamond anvil cell at room temperature on the ID09A beamline in the European Synchrotron Radiation Facility (Grenoble, France). A 4:1 by volume mixture of methanol and ethanol was utilized as pressure transmitting medium. Monochromatic radiation at 0.4133 Å was used for pattern collection on image plates. The images were integrated using the program FIT2D [16] to yield intensity versus 2θ diagrams. The ruby luminescence method [17] was used for pressure calibration.

High-pressure time-of-flight neutron powder diffraction patterns of $PbWO_4$ and $BaWO_4$ were collected on the Pearl diffractometer at ISIS (Rutherford Appleton Laboratory, UK) using the Paris–Edinburgh pressure cell [18]. The samples were loaded into TiZr encapsulated gaskets, along with small amounts of 4:1 by volume mixture of deuterated methanol:ethanol mixture to act as a pressure transmitting medium [19]. The pressures for $PbWO_4$ were determined from the equation of state (EoS) by Hazen *et al* [20], $B_0 = 64(2)$ GPa and $B' = 4.0$. The pressures for $BaWO_4$ were extracted from the EoS by Panchal *et al* [6], $B_0 = 57$ GPa and $B' = 3.5$.

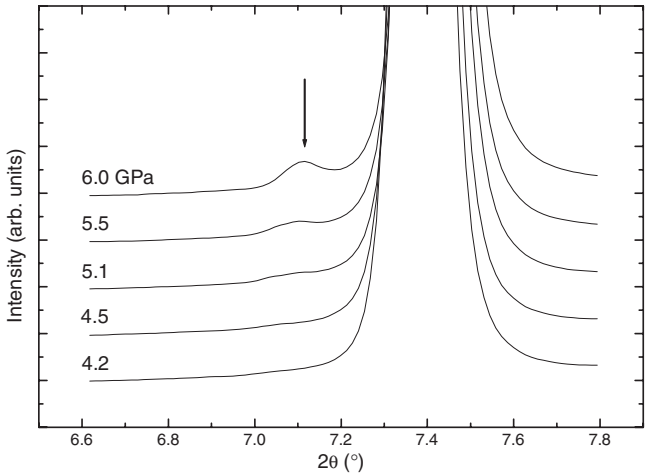

Figure 2. X-ray powder patterns of $PbWO_4$ in the 2θ range between 6.6° and 7.8°, collected from 4.2 to 6.0 GPa ($\lambda = 0.4133$ Å). The arrow indicates the appearance of a new non-scheelite reflection. The numbers stand for pressures in GPa.

3. Results and discussion

X-ray diffraction patterns of $PbWO_4$ collected in a diamond anvil cell at different pressures and room temperature are shown in figure 1. Upon compression to 4.5 GPa, the stable structure is of the scheelite type ($I4_1/a$, $Z = 4$). At higher pressures (figures 1 and 2), new weak reflections occur that cannot be accounted for with the fergusonite ($I2/a$, $Z = 4$), $PbWO_4$-III ($P2_1/n$, $Z = 8$), $LaTaO_4$ ($P2_1/c$, $Z = 4$), $HgWO_4$ ($C2/c$, $Z = 4$), or $BaMnF_4$ ($Cmc2_1$, $Z = 4$) types previously considered as candidates for the pressure-induced post-scheelite structures [7, 21]. In fact, the reflections due to the scheelite structure ($I4_1/a$, $Z = 4$) are still detectable to at least 10 GPa. However, the reflections of the new phase are significantly broadened and poorly resolved so that the structure determination is not feasible. Upon decompression, the new crystalline material transforms back to the scheelite structure (figure 1), excluding the possibility of pressure-induced decomposition, previously found in $SrWO_4$ [9].

High-pressure room-temperature time-of-flight neutron powder diffraction patterns of $PbWO_4$ and $BaWO_4$ are presented in figures 3 and 4, respectively. The patterns of $PbWO_4$ up to the cell load of 50 tonnes and the pressure of 4.9 GPa could be refined with the model of the scheelite structure using the Rietveld method [22] (figures 3 and 5, table 1). At higher loads (pressures), the patterns dramatically lose their intensity and are no longer useful for any refinements or analysis. Such behaviour corresponds to the progressive formation of the transformed, if not (partially) amorphous, $PbWO_4$ material as evidenced in the x-ray data (figures 1 and 2). Similar observations could be made in the case of $BaWO_4$ above 66 tons and 5.4 GPa (figures 4 and 6, table 2). Over the pressure range in which the $BaWO_4$ fergusonite polymorph ($I2/a$, $Z = 4$) is stable (above 7 GPa) [6], the observed Bragg intensities in the neutron powder patterns are very weak (figure 5).

The selected results of Rietveld refinements of the neutron powder patterns of $PbWO_4$ and $BaWO_4$ scheelites ($I4_1/a$, $Z = 4$) are given in figure 7 and tables 1 and 2. Both compounds have similar pressure dependences of interatomic distances and bond angles (figure 7). Their compressibilities are primarily due to shortening of the Pb–O or Ba–O bonds rather than to the

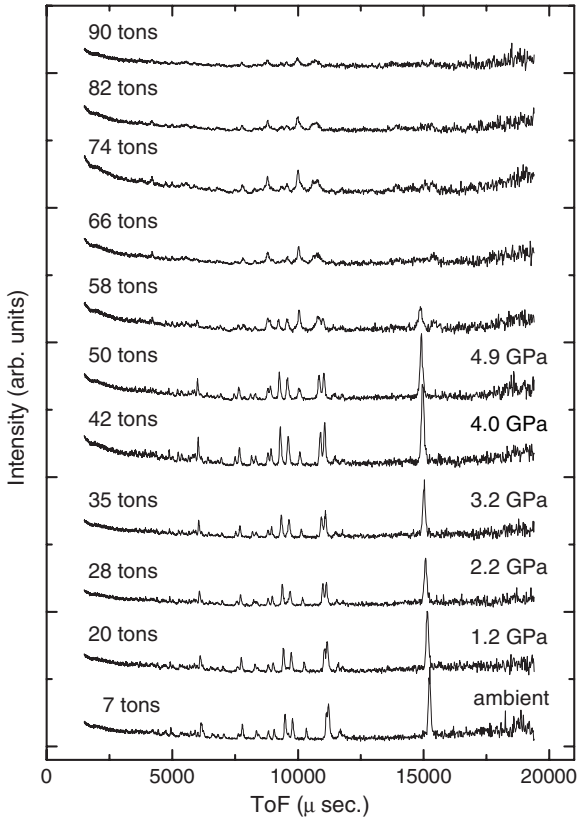

Figure 3. Time-of-flight neutron powder diffraction patterns of $PbWO_4$. The numbers stand for the hydraulic loads in tons and pressures in GPa.

changes of the W–O bonds in the WO_4^{2-} tetrahedral units. The intratetrahedral bond angles O–W–O are not significantly sensitive to pressures, while the interpolyhedral W–O–Me angles (Me: Pb or Ba) tend to converge upon compression. Bulk moduli (K_p) for the BaO_8 and PbO_8 polyhedra as well as for the WO_4^{2-} tetrahedra could be estimated from the formula proposed by Hazen *et al* [20]: $K_p = 750Z/d^3$, where Z is a formal cation charge and d is a mean cation–oxygen bond distance. The K_p values for the BaO_8 and PbO_8 polyhedra in $BaWO_4$ and $PbWO_4$ are 72 and 83 GPa, respectively. They are fairly close to the B_0 parameters in their equations of state ($BaWO_4$: $B_0 = 57$ GPa [6]; $PbWO_4$: $B_0 = 64$ GPa [20]). The tetrahedral WO_4^{2-} bulk moduli for $BaWO_4$ and $PbWO_4$ are 800 and 794 GPa, respectively.

When the cationic sublattice in the scheelite structure is considered, each of the cations has four nearest neighbours of the same type and eight nearest neighbours of the other type. All the intercationic distances are exactly equal in the fluorite structure. The ideal arrangement of the cations is favoured by their repulsive interactions, while the tetragonal distortion is induced by the packing of the anions [23]. It is evident in figure 8 that the differences between the W–Pb′ and W–Pb″ nearest-neighbour distances in $PbWO_4$ as well as between the W–Ba′ and W–Ba″ ones in $BaWO_4$ decrease with pressure. This observation, together with the decrease of the c/a axial ratios in tungstate scheelites [6, 7, 9, 20, 21], demonstrates that the tetragonal distortions in the cationic sublattices in both materials $PbWO_4$ and $BaWO_4$ are diminished at high pressures.

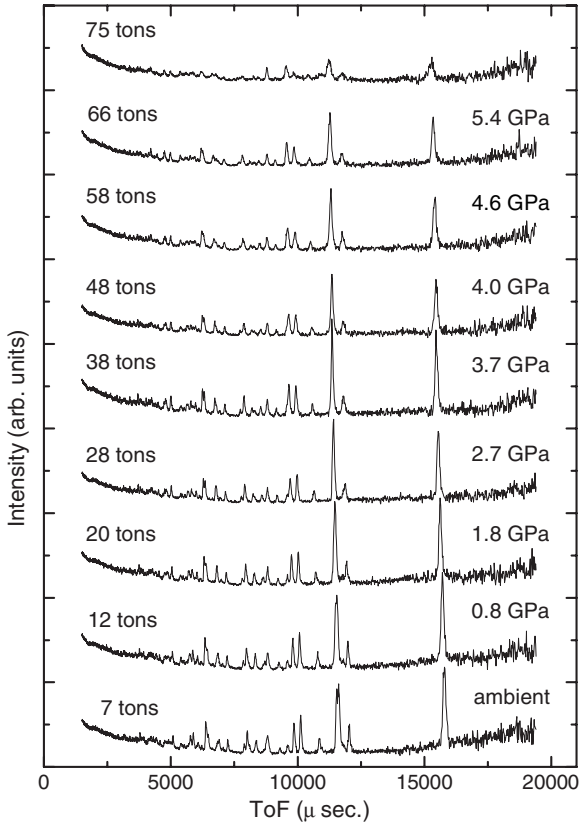

Figure 4. Time-of-flight neutron powder diffraction patterns of $BaWO_4$. The numbers stand for the hydraulic loads in tons and pressures in GPa.

The compressibility of scheelite-type $BaWO_4$ and $PbWO_4$ could further be analysed by considering the eight-coordinated BaO_8 and PbO_8 polyhedra in both materials (figures 9 and 10). The oxygen–oxygen distances around the Ba atoms in $BaWO_4$ are more sensitive to increasing pressure than the corresponding distances around the Pb atoms in $PbWO_4$ (figure 10). The most striking feature in figure 10 is the pressure-induced elongation of the O(5)–O(6) distances in $BaWO_4$ that are perpendicular to the c axis, while the respective O(5)–O(6) distances in $PbWO_4$ slightly decrease upon compression. It is worth noticing that the corresponding oxygen–oxygen distances in $CaMoO_4$ are effectively constant between atmospheric pressure and 5.7 GPa [20]. Our observations documented in figure 10 indicate that the distortions of the polyhedra around the Ba and Pb atoms in $BaWO_4$ and $PbWO_4$, respectively, are distinct and lead to different deformations of the anionic sublattices in the two materials.

The pressure dependence of structural distortions in the scheelite structure, especially in its anionic sublattice, could also be described by pseudosymmetry that is indicative of a slightly distorted structure of higher symmetry. If the distortion is small enough, it can be expected that the material would tend to acquire a more symmetric structure as a function of pressure and/or temperature [14]. For this purpose, we used the refined structural data of $PbWO_4$ and $BaWO_4$ from the neutron powder patterns in the program PSEUDO of the Bilbao Crystallographic Server [15]. The $I4_1/a$ space group of the scheelite structure is a

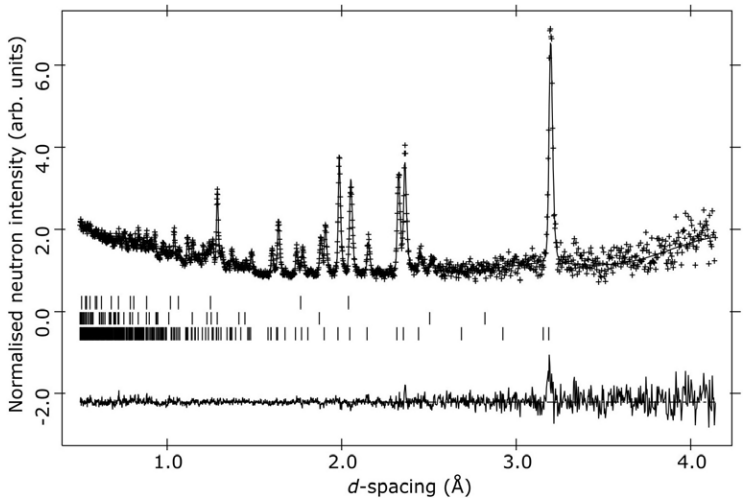

Figure 5. Observed, calculated, and difference neutron powder diffraction patterns of $PbWO_4$ ($I4_1/a$, $Z = 4$) at 4.0 GPa. Vertical markers indicate the Bragg reflections of $PbWO_4$ (bottom), WC (middle), and Ni (top). The weak reflections from WC and Ni arise from the anvils of the pressure cell.

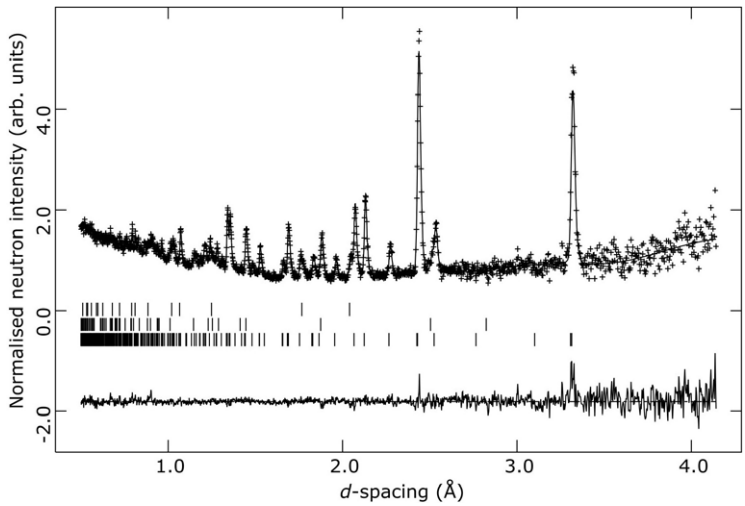

Figure 6. Observed, calculated, and difference neutron powder diffraction patterns of $BaWO_4$ ($I4_1/a$, $Z = 4$) at 2.7 GPa. Vertical markers indicate the Bragg reflections of $BaWO_4$ (bottom), WC (middle), and Ni (top). The weak reflections from WC and Ni arise from the anvils of the pressure cell.

subgroup of index 24 with respect to the space group $Fm\bar{3}m$, which represents the symmetry of the ideal fluorite structure. Three possible chains of maximal subgroups are involved in the $Fm\bar{3}m \rightarrow I4_1/a$ group–subgroup relationship. Assuming the Δ-criterion of 1 Å as a maximum distance (see [14, 15] for definition), the only pseudosymmetry encountered for the two structures is with respect to $I4_1/amd$ in the chain of maximal subgroups $Fm\bar{3}m \rightarrow I4/mmm \rightarrow P4_2/nnm \rightarrow I4_1/amd \rightarrow I4_1/a$. The calculated relative atomic displacements from the higher symmetrical symmetry of space group $I4_1/amd$ are shown in figure 11. In both

Table 1. Structure parameters and agreement factors from the Rietveld refinement of the neutron powder diffraction pattern for $PbWO_4$ collected at 4.0 GPa—$I4_1/a$, $Z = 4$, $a = 5.3851(3)$ Å, $c = 11.7223(10)$ Å, $V = 339.94(4)$ Å^3.

x(O)	0.2303(6)
y(O)	0.1007(5)
z(O)	0.0406(3)
U_{iso} (Pb)	0.0152(13)
U_{iso}(W)	0.0113 (18)
U_{iso}(O)	0.0152(11)
Interatomic distances (Å)	
W–O	1.779(3)
Pb–O	2.580(3)
	2.554(3)
Bond angles (deg)	
O–W–O	108.0(1)
	112.4(2)
W–O–Pb	132.6(2)
	120.7(2)
Agreement factors (%)	
R_p	7.50
wR_p	4.53

Table 2. Structure parameters and agreement factors from the Rietveld refinement of the neutron powder diffraction pattern for $BaWO_4$ collected at 2.7 GPa—$I4_1/a$, $Z = 4$, $a = 5.5423(4)$ Å, $c = 12.4433(15)$ Å, $V = 382.22(6)$ Å^3.

x(O)	0.2316(6)
y(O)	0.1191(5)
z(O)	0.0453(3)
U_{iso}(Ba)	0.0113(14)
U_{iso}(W)	0.0102 (16)
U_{iso}(O)	0.0155(10)
Interatomic distances (Å)	
W–O	1.777(4)
Ba–O	2.717(3)
	2.689(4)
Bond angles (deg.)	
O–W–O	108.1(1)
	112.2(2)
W–O–Ba	136.8(2)
	120.0(2)
Agreement factors (%)	
R_p	7.56
wR_p	4.59

scheelite materials ($I4_1/a$, $Z = 4$), all the cations are located at ideal positions so that only the oxygen atoms are responsible for the lowering of the symmetry to $I4_1/a$ [23]. It is remarkable

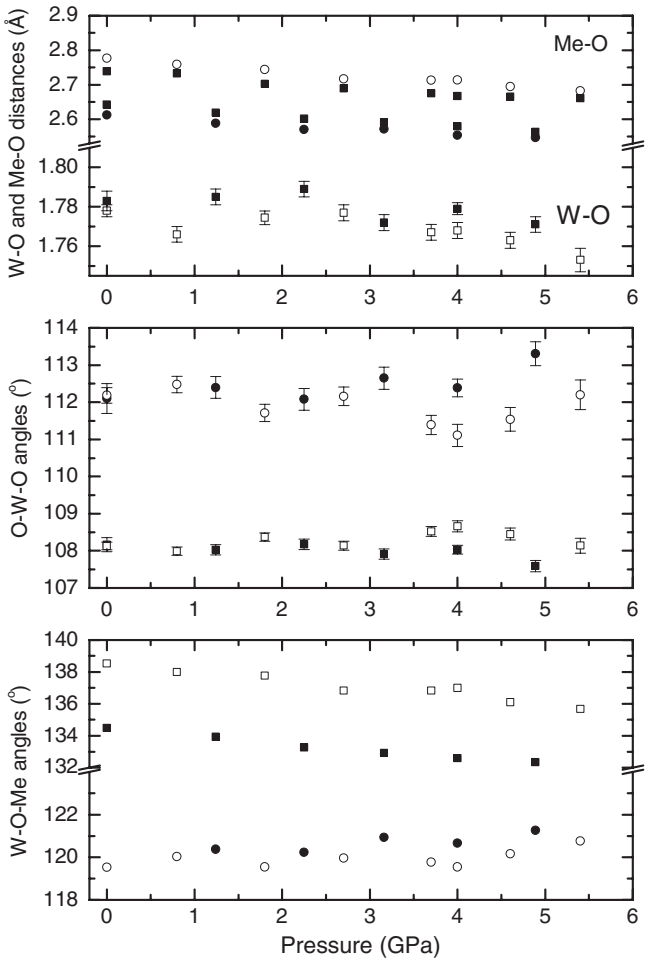

Figure 7. Pressure dependence of interatomic distances W–O, Me–O and bond angles O–W–O, W–O–Me in $PbWO_4$ (full symbols) and $BaWO_4$ (open symbols), Me = Pb or Ba, respectively. Error bars are shown when larger than the sizes of data points.

that the pressure dependences of the relative oxygen displacements in $PbWO_4$ and $BaWO_4$ are just opposite. The deviation from the higher symmetrical space group in the anionic sublattice of barium tungstate is enhanced with increasing pressure while, on the other hand, the degree of pseudosymmetry in lead tungstate increases.

4. Conclusions

The results of this study provide evidence that the compressibility in $PbWO_4$-I and $BaWO_4$-I (both $I4_1/a$, $Z = 4$) is dominated by the large pressure dependence of the Pb–O and Ba–O distances relative to the W–O bond lengths, since the WO_4^{2-} tetrahedra in both materials are effectively rigid and isolated structural units. Scheelites $CaWO_4$ [7], $SrWO_4$ [9], $BaWO_4$ [6], and $PbWO_4$ [20] are more compressible along the c axis. However, the high-pressure structures above 10, 10.5, 6.5, and 4.5 GPa in $CaWO_4$ [7], $SrWO_4$ [9], $BaWO_4$ [6], and $PbWO_4$ (this study) respectively seem to be different. The first three compounds transform to the fergusonite

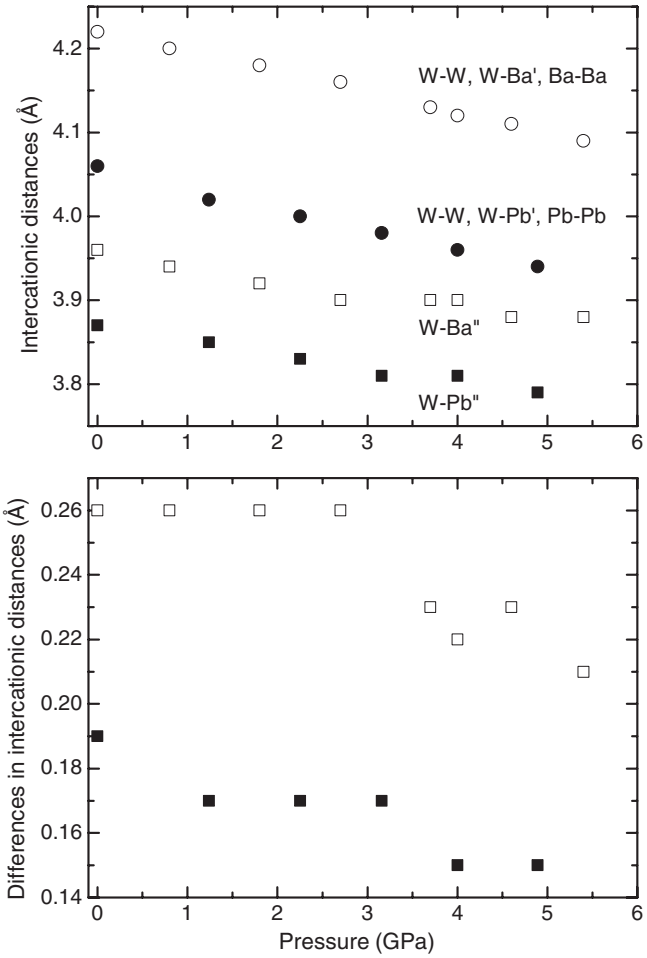

Figure 8. Pressure dependence of intercationic distances and their differences in $PbWO_4$ (full symbols) and $BaWO_4$ (open symbols).

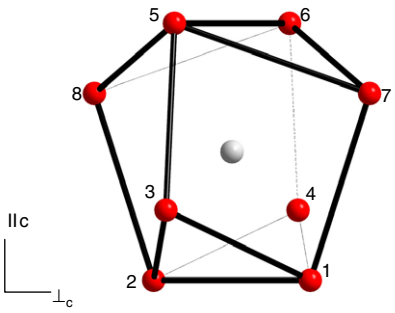

Figure 9. Eight-coordinated polyhedron in $BaWO_4$ at ambient pressure. The unique axis is vertical. The numbers label the oxygen atoms around the central atom.

structure ($I2/a$, $Z = 4$), that is a distorted variant of the scheelite type. Our observations show that the distortion in the anionic array from the ideal fluorite packing in $BaWO_4$-I increases

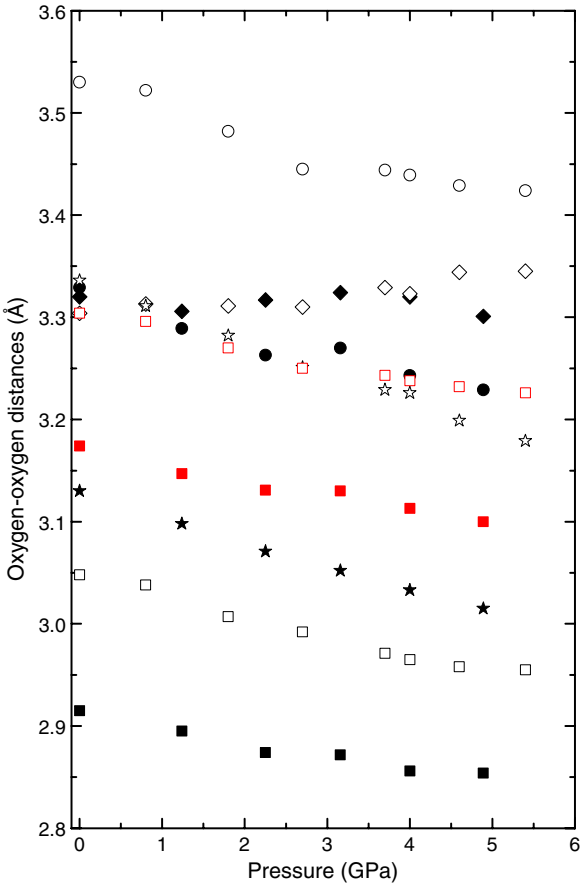

Figure 10. Pressure dependence of oxygen–oxygen distances in the eight-coordinated polyhedra in $BaWO_4$ (open symbols) and $PbWO_4$ (full symbols). Black squares, circles, diamonds, and stars stand for the distances O(5)–O(8), O(5)–O(7), O(5)–O(6), and O(5)–O(3), respectively (see figure 9 for oxygen atom labels). Red squares represent average oxygen–oxygen distances. The slopes of the fitted lines (not shown for clarity) to the O(5)–O(8), O(5)–O(7), O(5)–O(6), and O(5)–O(3) distances for $BaWO_4$($PbWO_4$) are −0.018 85 (−0.012 74), −0.021 24 (−0.018 98), 0.007 47 (−0.001 32), and −0.028 74 (−0.023 54), respectively.

upon compression (figure 11), eventually resulting in the monoclinic derivative of the ideal fluorite [6]. On the other hand, the pseudosymmetry of $PbWO_4$-I stolzite ($I4_1/a$, $Z = 4$) with respect to its minimal supergroup ($I4_1/amd$, $Z = 4$) increases (figure 11), suggesting that the high-pressure phase could have higher symmetry than $I4_1/a$ or that the fluorine sublattice is less distorted in the high-pressure phase. Unlike in $SrWO_4$ [9], no indications for decomposition of the $PbWO_4$ material are found in this study.

It has already been shown that the systematics and the competition between pressure-induced structural instabilities of the scheelite or fergusonite polymorphs (including their decomposition) in the ABX_4 family depend on the ionic radii [7, 19, 24]. For instance, the phase transition pressures may be correlated with the relative sizes of the A and BX_4 ions [19]. In addition, depending on the size of the M^{3+} cation in the $LiMF_4$ scheelites, they transform to fergusonites and/or decompose [24]. The compressibility of $PbWO_4$ scheelite, in which the pseudosymmetry increases, cannot be explained on the basis of the relative sizes of the

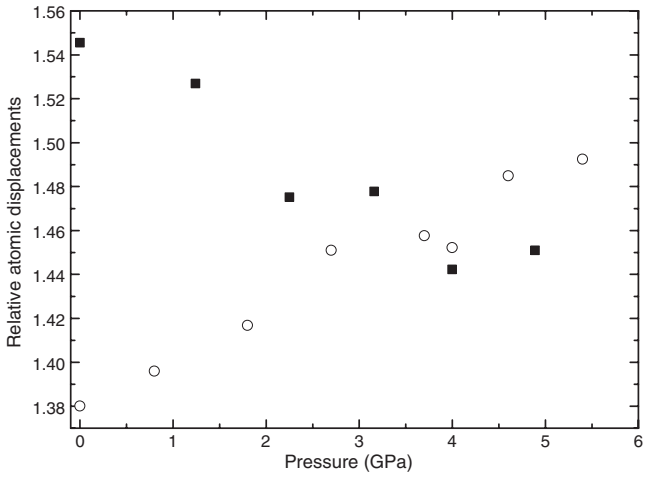

Figure 11. Relative atomic displacements of the oxygen atoms in the scheelite ($I4_1/a$, $Z = 4$) structures of $PbWO_4$ (full symbols) and $BaWO_4$ (open symbols) with respect to space group $I4_1/amd$ ($Z = 4$) calculated with the program PSEUDO [15].

Me^{2+} cations in the series of $MeWO_4$ scheelite-structured compounds (Me: Ca, Sr, Ba, or Pb). It is, then, an open question whether the stereochemical activity on the non-bonding electron pair in the Pb^{2+} cation has any influence on the $PbWO_4$ polymorphism at high pressures and high temperatures.

Acknowledgments

The x-ray data were collected during the HS-2120 beamtime at ID09A, ESRF. The neutron data were measured during the RB15330 beamtime at HiPr/Pearl, ISIS. We thank D J Francis for his technical assistance at ISIS. AG and KF acknowledge financial support from the Ministerio de Ciencia y Tecnología, Ministerio de Educación y Cultura, and Gobierno Vasco.

References

[1] Nistor S V, Stefan M, Goovaerts E, Nikl M and Bohacek P 2006 *J. Phys.: Condens. Matter* **18** 719
Stefan M, Nistor S V, Goovaerts E, Nikl M and Bohacek P 2005 *J. Phys.: Condens. Matter* **17** 719
[2] Fujita T, Kawada I and Kato K 1977 *Acta Crystallogr.* B **33** 162
[3] Jayaraman A, Batlogg B and VanUitert L G 1983 *Phys. Rev.* B **28** 4774
[4] Jayaraman A, Batlogg B and VanUitert L G 1985 *Phys. Rev.* B **31** 5423
[5] Christofilos D, Ves S and Kourouklis G A 1996 *Phys. Status Solidi* b **198** 539
Christofilos D, Papagelis K, Ves S, Kourouklis G A and Raptis C 2002 *J. Phys.: Condens. Matter* **14** 12641
[6] Panchal V, Garg N, Chauhan A K, Sangeeta B and Sharma S M 2004 *Solid State Commun.* **130** 203
[7] Grzechnik A, Crichton W A, Hanfland M and van Smaalen S 2003 *J. Phys.: Condens. Matter* **15** 7261
[8] Crichton W and Grzechnik A 2004 *Z. Kristallogr. NCS* **219** 337
[9] Grzechnik A, Crichton W A and Hanfland M 2005 *Phys. Status Solidi* b **242** 2795
[10] Christofilos D, Arvanitidis J, Kampasakali E, Papagelis K, Ves S and Kourouklis G A 2004 *Phys. Status Solidi* b **241** 3155
[11] Kawada I, Kato K and Fujita T 1974 *Acta Crystallogr.* B **30** 2069
[12] Richter P W, Kruger G J and Pistorius C W F T 1976 *Acta Crystallogr.* B **32** 928
[13] Li S, Ahuja R, Wang Y and Johansson B 2003 *High Pressure Res.* **23** 343
[14] Kroumova E, Aroyo M I and Pérez-Mato J M 2002 *Acta Crystallogr.* B **58** 921

[15] http://www.cryst.ehu.es/
Kroumova E, Aroyo M I, Perez-Mato J M, Ivantchev S, Igartua J M and Wondratschek H 2001 *J. Appl. Crystallogr.* **34** 783
[16] Hammersley A P, Svensson S O, Hanfland M, Fitch A N and Häusermann D 1996 *High Pressure Res.* **14** 235
[17] Piermarini G J, Block S, Barnett J D and Forman R A 1975 *J. Appl. Phys.* **46** 2774
Mao H K, Xu J and Bell P M 1986 *J. Geophys. Res.* **91** 4673
[18] Besson J M, Nelmes R J, Hamel G, Loveday J S, Weill G and Hull S 1992 *Physica* B **180** 907
[19] Marshall W G and Francis D J 2002 *J. Appl. Crystallogr.* **35** 122
[20] Hazen R M, Finger L W and Mariathasan J W E 1985 *J. Phys. Chem. Solids* **46** 253
[21] Errandonea D, Manjón F J, Somayazulu M and Häusermann D 2004 *J. Solid State Chem.* **177** 1087
[22] Larson A C and von Dreele R B 2000 *GSAS: General Structure Analysis System* Los Alamos National Laboratory
[23] Hyde B G and Andersson S 1989 *Inorganic Crystal Structures* (New York: Wiley)
[24] Grzechnik A, Friese K, Dmitriev V, Weber H-P, Gesland J-Y and Crichton W A 2005 *J. Phys.: Condens. Matter* **17** 763